Cell and Molecular Biology: Open Access
Received: Jun 27, 2016, Accepted: Aug 01, 2016, Published: Aug 05, 2016
Cell Mol Biol, Volume 2, Issue 1
http://crescopublications.org/pdf/cmboa/CMBOA-2-009.pdf
Article Number: CMBOA-2-009

Research Article Open Access

MMP InhibitionInduces Mesenchymal-Epithelial Transition of Human Osteosarcoma Cells

Kinga Vojnits[1,2*], Chen Fu[3*], Andrea Hayes-Jordan[1,4],Yong Li[1,2#]

[1]Department of Pediatric Surgery, University of Texas Medical School at Houston, TX 77030, USA
[2]Center for Stem Cell and Regenerative Medicine, University of Texas Health Science Center at Houston (UTHealth), TX 77030, USA
[3]University of Texas Medical School at Houston, TX 77030, USA
[4]Surgery and Pediatrics University of Texas MD Anderson Cancer Center, TX 77030, USA

#Corresponding Author: Yong Li, MD. PhD, Center for Stem Cell and Regenerative Medicine, University of Texas Health Science Center at Houston (UTHealth),1825 Pressler Street, Houston, TX 77030, USA; Tel: +1 (713) 500-2438; E-mail: yong.li.1@uth.tmc.edu

***Equal contribution.**

Citation: KingaVojnits, Chen Fu, Andrea Hayes-Jordan and Yong Li (2016) MMP Inhibition Induces Mesenchymal-Epithelial Transition of Human Osteosarcoma Cells. Cel Mol Biol 2: 009.

Abstract

Osteosarcoma is the most common malignant solid tumor that is extremely prone to metastasis. However, the mechanism for this increased metastatic potential has yet to be fully clarified. Undifferentiated cancers are significantly more malignant than their well differentiated counterparts. It has been considered that osteosarcoma cells overexpress matrixmetalloproteinases (MMPs), a group of extracellular degradation proteins. We attempt to resolve the essential role that MMPs play in the metastatic potential of osteosarcomas. Our hypothesis is that MMP inhibition will abrogate the mesenchymal phenotype, which will subsequently lead to an attenuated metastatic potential. We discovered that MMP inhibition not only decreased the gene and protein expression of several mesenchymal markers, such as N-Cadherin, but also increased the expression of the epithelial markers, such as E-Cadherin and Cytokeratins. Furthermore, we observed a diminished cell migration potential upon MMP inhibition *in vitro*. Our study suggests that the simultaneous presence of attenuated mesenchymal phenotype and decreased cell migration potential in the presence of MMP inhibition may provide additional mechanistic evidence and a novel perspective in cancer cells.

Keywords: MMP inhibition; Mesenchymal-epithelial transition; Cell migration.

.

Introduction

Osteosarcoma is a malignant mesenchymal neoplasm that is extremely prone to metastasis, with over 80 percent of patients having metastatic disease at the time of diagnosis[1]. However, the mechanism for this increased metastatic potential has yet to be fully resolved[2]. It has long been known that osteosarcoma cells overexpress matrixmetalloproteinases (MMPs)[1], which belong to a family of zinc-dependent endopeptidases that play a major role in the degradation of extracellular proteins, as well as in various cell signaling pathways including apoptosis[3-5]. These MMPs are intimately involved in the malignant potential of these cancer cells[6-11] and, while it is generally accepted that much of this role can be attributed to the MMPs' degradatory properties, further signaling involvement is steadily being elucidated[3-6, 8-17]. There are over 28 different MMP enzymes with unique functions and locations within the cellular environment. MMP1, also known as interstitial collagenase and fibroblast collagenase, is involved in the degradation of interstitial collagens I, II and III.MMP1 is secreted following the interaction between α2β1 integrin and dermal fiber type I collagen and the subsequent induction of ERK signaling[6]. MMP1 has known involvement in a myriad of disease processes, including cancer metastasis[6, 11]. Moreover, several studies have linked increased MMP1 secretion with poor disease prognosis and increased migratory capacity[6, 8, 9, 11, 16]. In this experiment, we attempt to elucidate new information regarding MMP inhibition, including MMP1 inhibition, and its role in decreasing the migratory potential of osteosarcoma cells, and delineate a potential link between this attenuation of migratory potential and an abrogation of the cell's undifferentiated mesenchymal characteristics.

Undifferentiated cancers are significantly more prone to malignancy and treatment-resistant than their well-differentiated counterparts, and so determining themechanism behind the expansion of undifferentiated cells within a tumor microenvironment is of particular interest to both scientists and clinicians. One of the more prominent hypothesesthat seeks to explain the mechanism by which cells achieve this expansion is through a phenomenon known as Epithelial-Mesenchymal Transition (EMT), which was originally discovered in chick embryogenesis but is now known to occur in a variety of different cancers, such as GI and pancreatic cancers[18, 19]. In EMT, polarized epithelial cells undergo a sequence of biochemical and biophysical changes, which cause them, exhibit a more mesenchymal nature. In cancers, this is particularly problematic, as mesenchymal cells are more invasive, malignant, and resistant to chemotherapeutic agents than their epithelial counterparts[20-22]. Osteosarcoma cells are mesenchymal in nature and normally differentiate into the osteoblasticlineage. However, it has recently been discovered that osteosarcoma can be induced to undergo an EMT like phenomenon known as Mesenchymal-Epithelial Transition (MET)[16, 20, 22-28]. This phenomenon has consistently been associated with a decreased malignant capacity and a generally more docile phenotype[20, 28].While the phenomenon of EMT has been observed in many different cancer types, most notably breast, prostate, and GI, the reverse phenomenon of MET is not very well understood[7, 12, 16, 18-40].

In the current investigation we seek to delineate the link between migratory potential and mesenchymal phenotype in the context of MMPinhibition in osteosarcoma cells *in vitro*. Our hypothesis is that MMPs, including MMP1inhibition will abrogate the mesenchymal phenotype, which will subsequently lead to an attenuated migratory potential.

Materials and Methods

Cell Maintenance and Treatment

The primary human osteosarcoma cell line MG63 was obtained from ATCC (USA). Cells were cultured in growth media [Minimum Essential Media, 10% Fetal Bovine Serum, 1% antibiotics (all from GIBCO, USA)] at 5% CO_2 in 37°C. Experimental groups were cultured with the specific MMP inhibitor GM6001 (Sigma, USA) at concentrations of 50nM and 250nM for 6 and 12 hours.

Viability Testing using Resazurin Assay

The viability testing was performed in 24-well plates where each test concentration was performed in triplicates (technical replicates). At least 3 independent biological replicates were performed to assess the variations of the toxic response. The viability was assessed the day after plating the MG63 cells to ensure proper cell attachment. After 6 and 12 hours of exposure with the GM6001 at a concentration range from 0.003nM – 31250nM, the medium was discarded and substituted by 100µl of freshly prepared 10µg/ml solution of resazurin (Sigma, USA) in growth media. After an incubation of 2 hours at 37°C and 5% CO_2, the supernatant was transferred into an empty 96-well plate and the fluorescence signal was measured at a wavelength of 590nm with a TECAN Infinite® 200 microplate reader (TECAN, USA).

Singe Cell Migration

Target cell populations and control cells were plated separately on 6-well plates, 10,000 cells/well, in growth media, 48 hours prior to the time-lapse experiment. Target MG63 cells were exposed to 50nM and 250nM GM6001 for 12 hours prior to the recording.

Time lapse images were acquired with an Andor IXon3 885 EMCCD camera (Andor, USA) on an Olympus IX-81 (Olympus, USA) microscope fitted with a microscope enclosure (Precision Plastics, USA), and images of single cell migration were taken for 6 hours at 3 minute intervals; 3 different fields/well were chosen for the recording. Proper environmental conditions were maintained in a micro incubator at 37 °C with 5% CO_2. A series of images were analysed using NIH ImageJ analysis software to track the centroid positions (x,y) of cell nuclei (which were assumed to be the representations of cell-bodies). Migration paths were plotted and analysed by the Chemotaxis and Migration Tool v2.0 from Ibidi. Net translocation distance was measured as the distance between the starting point and the end point of cells after 6 hours. Migration speed was calculated as total length of the migration path during the 6 hours period.

Immunohistochemistry

Samples were fixed with 4% paraformaldehyde (Sigma, USA) for 20 minutes at room temperature. After permeabilization with 0.2% Triton X-100 (Sigma, USA) for 30 minutes, nonspecific binding of antibodies was blocked for one hour with 10% BSA and 5% HS (Sigma, USA) in PBS, at room temperature. The primary antibodies (Table 1) were applied overnight at 4°C. After the overnight incubation, the cells were incubated for 1 hour at room temperature with the appropriate fluorescence-conjugated secondary antibodies (Table 1). The nuclei were revealed using 4', 6'-diamidino-2-phenylindole (DAPI) staining (Sigma, USA) and fluorescent microscopy (Nikon) was used to visualize the results. Quantitative image analysis was performed using the NIH ImageJ Software.

Table 1: Primary and secondary antibodies.

Primary antibodies	Host	Dilution	Manufacturer	Secondary antibodies
Cytokeratin 18	Mouse monoclonal IgG1	1:400	Santa Cruz	Goat anti-mouse Alexa Fluor 594
Cytokeratin 19	Goat polyclonal IgG	1:400	Santa Cruz	Donkey anti-goat Alexa Fluor 594
E cadherin	Rat monoclonal IgG1	1:400	Sigma	Goat anti-rat Alexa Fluor 594
N cadherin	Goat polyclonal IgG	1:400	Santa Cruz	Donkey anti-goat Alexa Fluor 594
α-smooth muscle actin	Mouse monoclonal IgG2a	1:500	Sigma	Goat anti-mouse Alexa Fluor 594
Vimentin	Goat polyclonal	1:500	Sigma	Donkey anti-goat Alexa Fluor 594

Quantitative Real-time PCR

Total RNA was isolated by using the RNeasy Plus Mini Kit (Quiagen, USA), and cDNA was synthesized from 1 µg of RNA *via* High Capacity RNA-to-cDNA Kit (Life Technologies, USA) following the manufacturer's instructions. Gene expression was analysed by quantitative real-time PCR **(**qPCR) using MyiQ real time PCR (Bio-Rad, USA). The applied primers (Table 2) were designed by Oligo software (Oligo Perfect Designer, Invitrogen, USA). Reactions were measured in duplicates using custom 2x Syber Green Master Mix based on the hot-start Jumpstart Taq DNA Polymerase enzyme (Sigma, USA). The amplification was done for 40 cycles (95°C 20 sec, 60°C 20 sec, 72°C 40 sec). To verify the PCR product, melting curves and negative controls were carried out in each reaction. Relative quantification of mRNA was determined by the ΔΔCt method ($2^{-\Delta\Delta Ct}$ formula) by using the expression profile of the corresponding control samples as reference.

Data Processing and Statistical Analysis

Prism 6.0 (GraphPad Software, USA) was used for data plotting, non-linear regression and statistical analysis. Data are given as mean ± S.E.M. Comparisons between two groups was performed by using Student's t-test assuming two-tailed distribution, and unequal variances. For multiple comparisons, ANOVA or Kruskal Wallis test was applied. Statistical significance was considered at $p<0.05$.

Table 2: PCR primers.

Gene	5'Primer	3'Primer
Cytokeratin 18	AGCGCCAGGCCCAGGAGTATGAGG	TATCCGGCGGGTGGTGGTCTTTTG
Cytokeratin 19	GCACTACAGCCACTACTACACGA	CTCATGCGCAGAGCCTGTT
E-cadherin	CAGAAAGTTTTCCACCAAAG	ACTGAACCTGACCGTACAAAATGTGAGCAATTCTGCT
N-cadherin	CTGGGACGTATGTGATGACG	TGATGATGTCCCCAGTCTCA
αSMA	CAAAGCCGGCCTTACAGAG	AGCCCAGCCAAGCACTG
Vimentin	GCAAAGATTCCACTTTGCT	GAAATTGCAGGAGGAGATGC
Gapdh	CACCCACTCCTCCACCTTT	CCACCACCCTGTTGCTGTA

Results

GM6001 Specifically Inhibits mRNA Expression of Several MMPs

In accordance to the literature, undifferentiated MG63 cells highly expressed several MMPs, such as MMP1, MMP2, MMP3, MMP9 and MMP14 as shown by our qPCR analysis (Figure 1). However, we did not see any expression of MMP7, MMP8, MMP12 and MMP26 in our cultured control cells (Figure 1).

Cell viability was defined after 6 and 12 hours exposure of GM6001 by using the resazurin reduction assay. In 3 biological replicates, concentration dependent cytotoxicity could be identified ranging from 0.003nM to 31250nM (Figure 2A). The data were used as a basis to define the highest non-cytotoxic concentration of GM6001, 50nM and 250nM that were applied for further experiments.

It has been shown that GM6001 is a specific inhibitor of MMP1, MMP2, MMP3, MMP7, MMP8, MMP9, MMP12, MMP14 and MMP26. Therefore, dose-response relationships were determined after 6 and 12 hours exposure of GM6001 by qPCR analysis (Figure 2). From all the tested MMPs, the MMP1 (Figure 2 B), MMP7 (Figure 2 E), MMP9 (Figure 2 G) and MMP14 (Figure 2 I) mRNA expression was the most sensitive to the treatment with the inhibitor, as already after 6 hours of exposure, their gene expression level was completely diminished at 50nM and higher concentrations. The mRNA expression of MMP2 (Figure 2 C), MMP3 (Figure 2 D), MMP8 (Figure 2 F) and MMP26 (Figure 2 J) was significantly decreased only after the 12 hours exposure of GM6001. Interestingly, the mRNA expression of MMP12 (Figure 2 H) was not affected by the inhibitor.

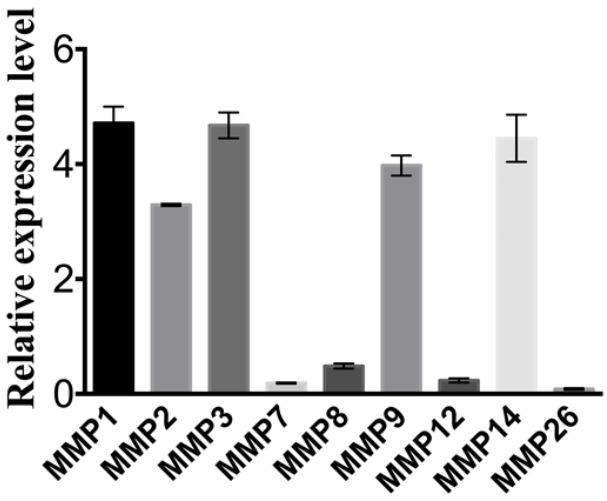

Figure 1: Gene expression of MMPs in the cultured undifferentiated MG63 cells.
QPCR analysis of the expression of MMPs in the undifferentiated control MG63 cells. Data were compared to Gapdh, and are presented as the mean ±SEM of 3 biological replicates.

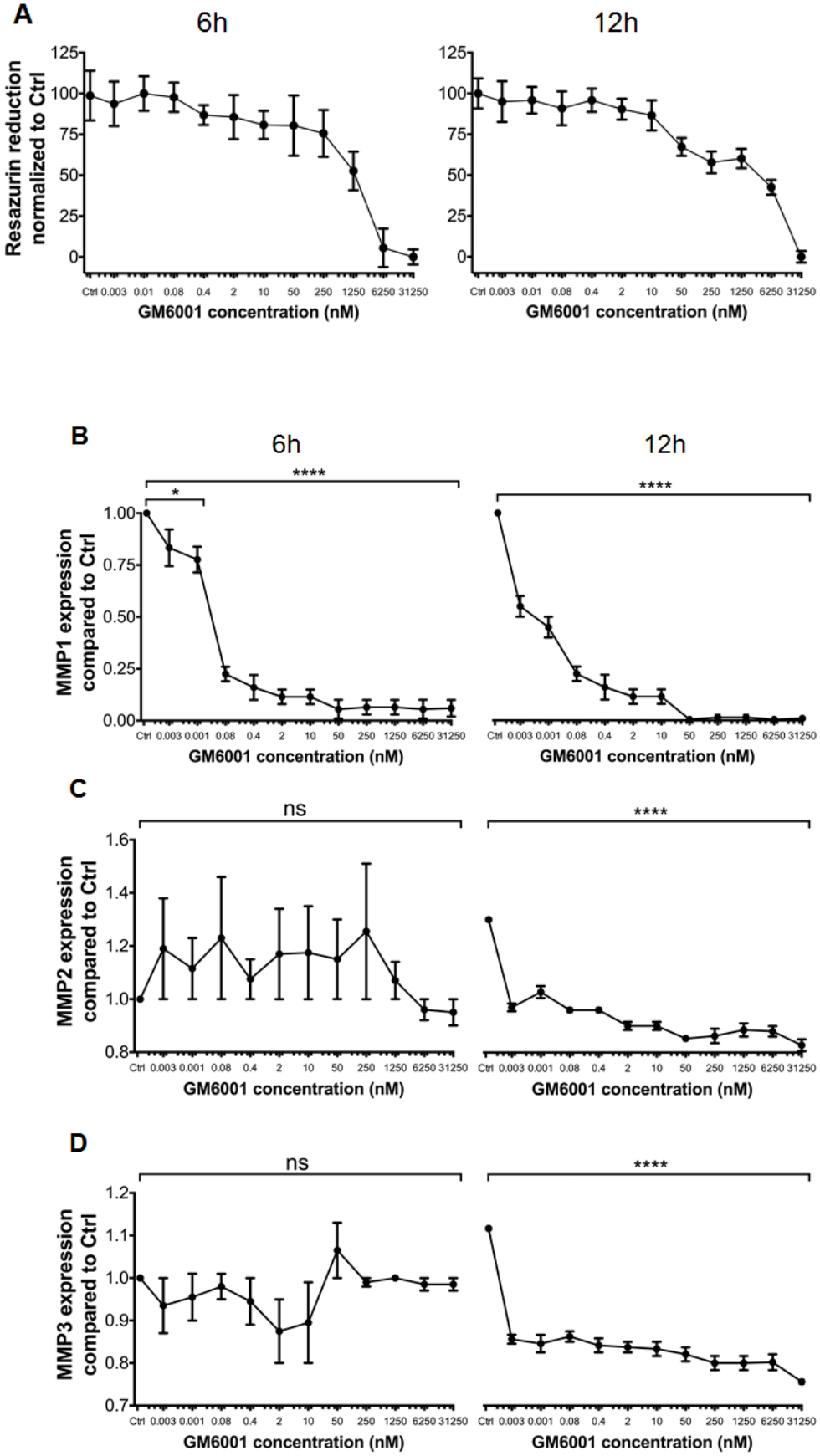
A
6h
12h
Resazurin reduction normalized to Ctrl
125
100
75
50
25
0
Ctrl 0.003 0.01 0.08 0.4 2 10 50 250 1250 6250 31250
GM6001 concentration (nM)
B
6h
12h
****
*
MMP1 expression compared to Ctrl
1.00
0.75
0.50
0.25
0.00
Ctrl 0.003 0.001 0.08 0.4 2 10 50 250 1250 6250 31250
GM6001 concentration (nM)
C
ns
****
MMP2 expression compared to Ctrl
1.6
1.4
1.2
1.0
0.8
D
MMP3 expression compared to Ctrl
1.2
1.1
1.0
0.9
0.8
0.7

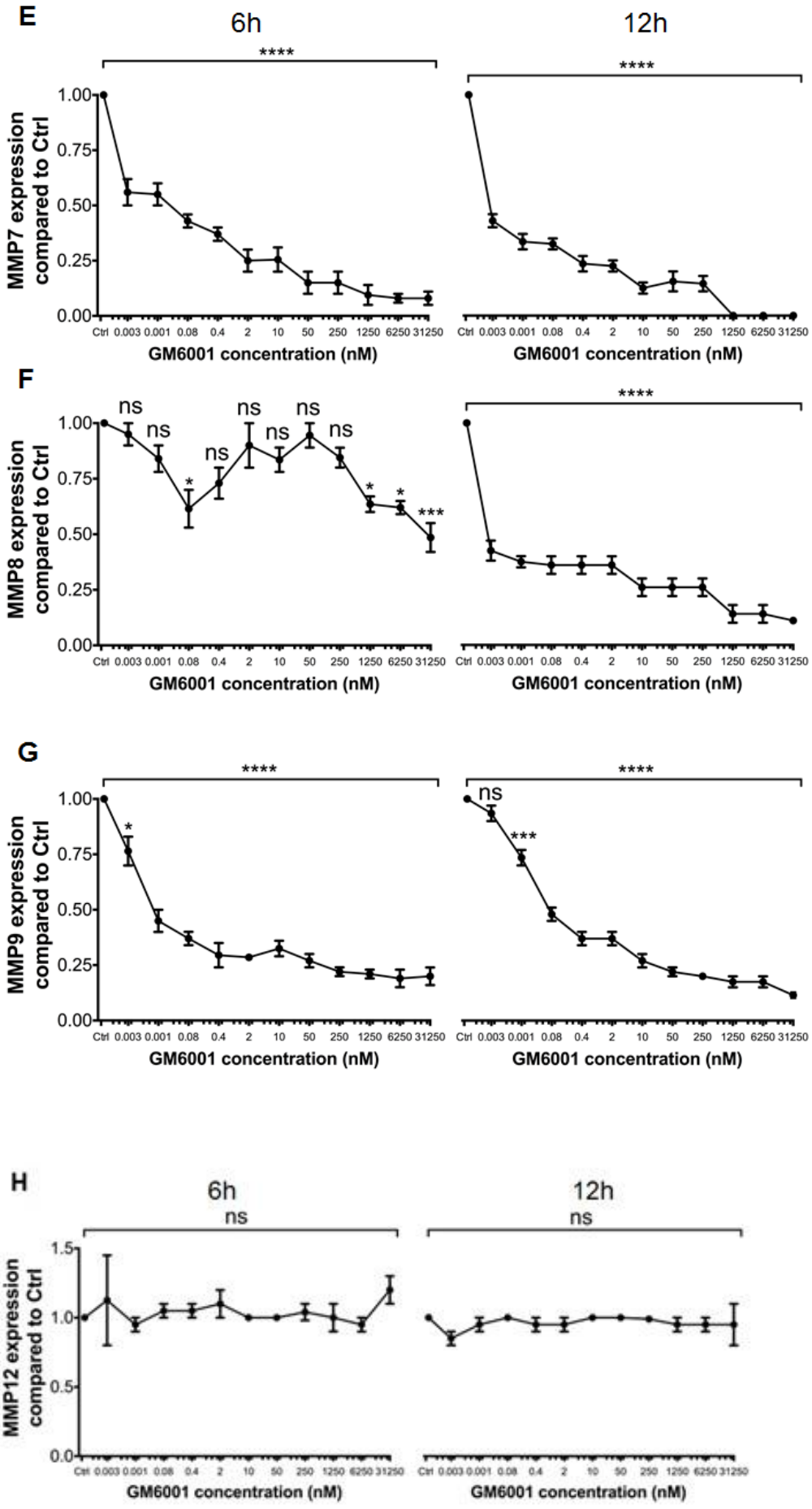
E
6h
12h
****
MMP7 expression compared to Ctrl
1.00
0.75
0.50
0.25
0.00
Ctrl 0.003 0.001 0.08 0.4 2 10 50 250 1250 6250 31250
GM6001 concentration (nM)
F
ns
*
***
MMP8 expression compared to Ctrl
G
MMP9 expression compared to Ctrl
H
MMP12 expression compared to Ctrl
1.5
1.0
0.5
0.0

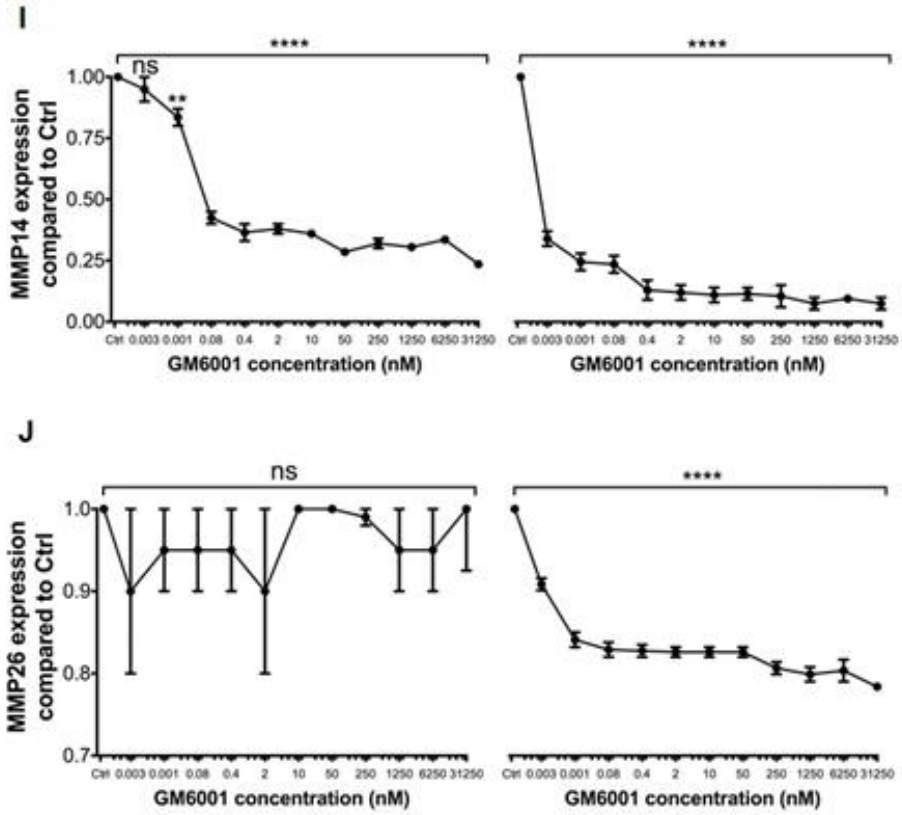

Figure 2: Inhibition of MMPs in MG63 cells by GM6001.

A) Resazurin based cytotoxicity.MG63 cells were exposed to 11 doses of GM6001 (0.003nM – 31250nM) for 6 and 12 hours. Each test concentration was performed in triplicates. Data are given as the mean ±SEM of 3 biological replicates. **B-J)** Inhibition of MMPs after 6 and 12 hours of treatment with GM6001. Data are presented as the mean ±SEM of 3 biological replicates. *P<0.05, **P<0.01, ***P<0.001, ****P<0.0001.

MMPInhibition Changes the Mesenchymal Phenotype of MG63 Sarcoma Cells *in vitro*

In order to prove our hypothesis that the MMP inhibition will retract the mesenchymal phenotype of cancers, MG63 cells were either treated with 50nM and 250nM MMP inhibitor, GM6001,for 6 and 12 hours. The cells were then fixed for immunofluorescence staining or collected for qPCR analysis.

The mRNA expression of the tested epithelial markers, such as E-cadherin, Cytokeratin 18, and Cytokeratin 19 (6.8±0.8 fold, 2.42±0.3 fold, 7.2±1.2 fold, respectively) was significantly increased after 6-hour 250nM GM6001 treatment (Figure 3 A). Only the Cytokeratin 19 expression was significantly upregulated (4.0±0.6 fold) at the 50nM GM6001 concentration (Figure 3 A). In contrast, the expression of the mesenchymal marker N-cadherin, α-smooth muscle actin (α-SMA) and Vimentin was significantly downregulated (0.47±0.08 and 0.17±0.04 fold, 0.8±0.1 and 0.66±0.1 fold, 0.53±0.12 and 0.35±0.08 fold, respectively) by both of the tested GM6001 concentrations (Figure 3 B). Similarly, the mRNA expression levels of the epithelial genes (Figure 3 C) were increased, while the mRNA expression levels of the mesenchymal marker genes (Figure 3 D) were decreased after 12 hour MMP inhibition. The upregulation of the epithelial genes were more pronounced (6.55±1.2 and 31.4±4 fold, 4.59±1 and 44.13±4.6 fold, 20.97±03.8 and 73.58±5.8 fold, respectively) after the 12-hour treatment, both at the tested concentrations. The effects on the mRNA downregulation of the mesenchymal markers were similar to the 6-hour treatment (0.3±0.08 and 0.05±0.02 fold, 0.75±0.2 and 0.34±0.07 fold, 0.44±0.1 and 0.26±0.06 fold, respectively).

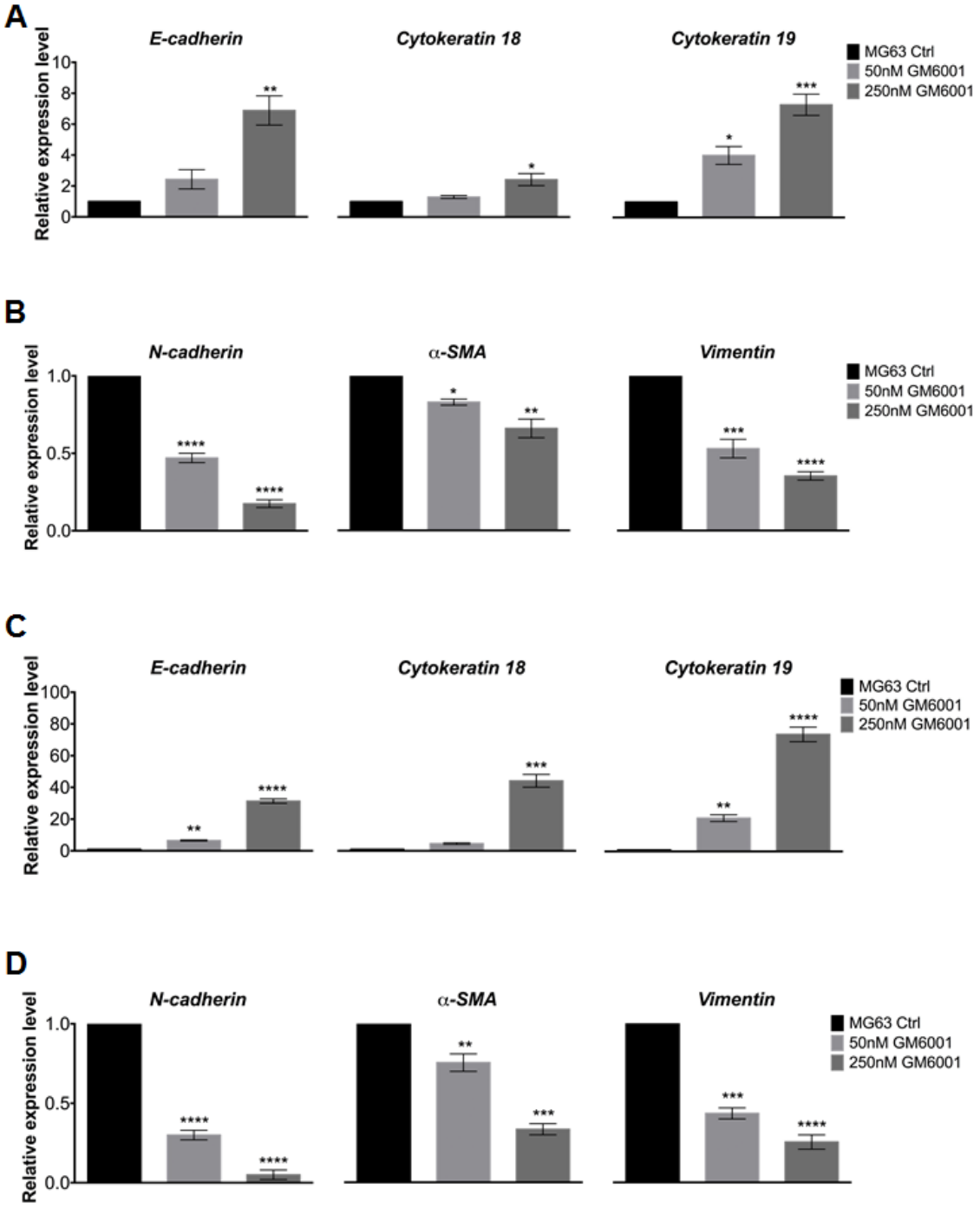

Figure 3: Changes in the epithelial and the mesenchymal gene expression profile of MG63 sarcoma cells by MMP inhibition. QPCR analysis of the expression of epithelial (**A**) and mesenchymal (**B**) marker genes after 6 hours GM6001 treatment, and the expression of epithelial (**C**) and mesenchymal (**D**) marker genes after 12 hours GM6001 treatment in the control and treated MG63 cells. Data were compared to the control cells, and are presented as the mean ±SEM of 3 biological replicates. *P<0.05, **P<0.01, ***P<0.001, ****P<0.0001.

The protein expression of the epithelial lineage markers, namely E-cadherin, Cytokeratin 18 and Cytokeratin 19 was significantly increased in the inhibitor treated cells (Figure 4 A). By measuring the cell signal intensity, we determined that the fluorescence intensities (Figure 4 B) became significantly higher upon MMP inhibition at both the tested concentrations after the 12-hour treatment. Correspondingly to the qPCR results, the protein expression of the mesenchymal lineage markers, N-cadherin, α-SMA and Vimentin became significantly decreased at both the tested concentrations after the 12-hour treatment (Figure 5 A). The measured fluorescence intensities are shown in Figure 5 B.

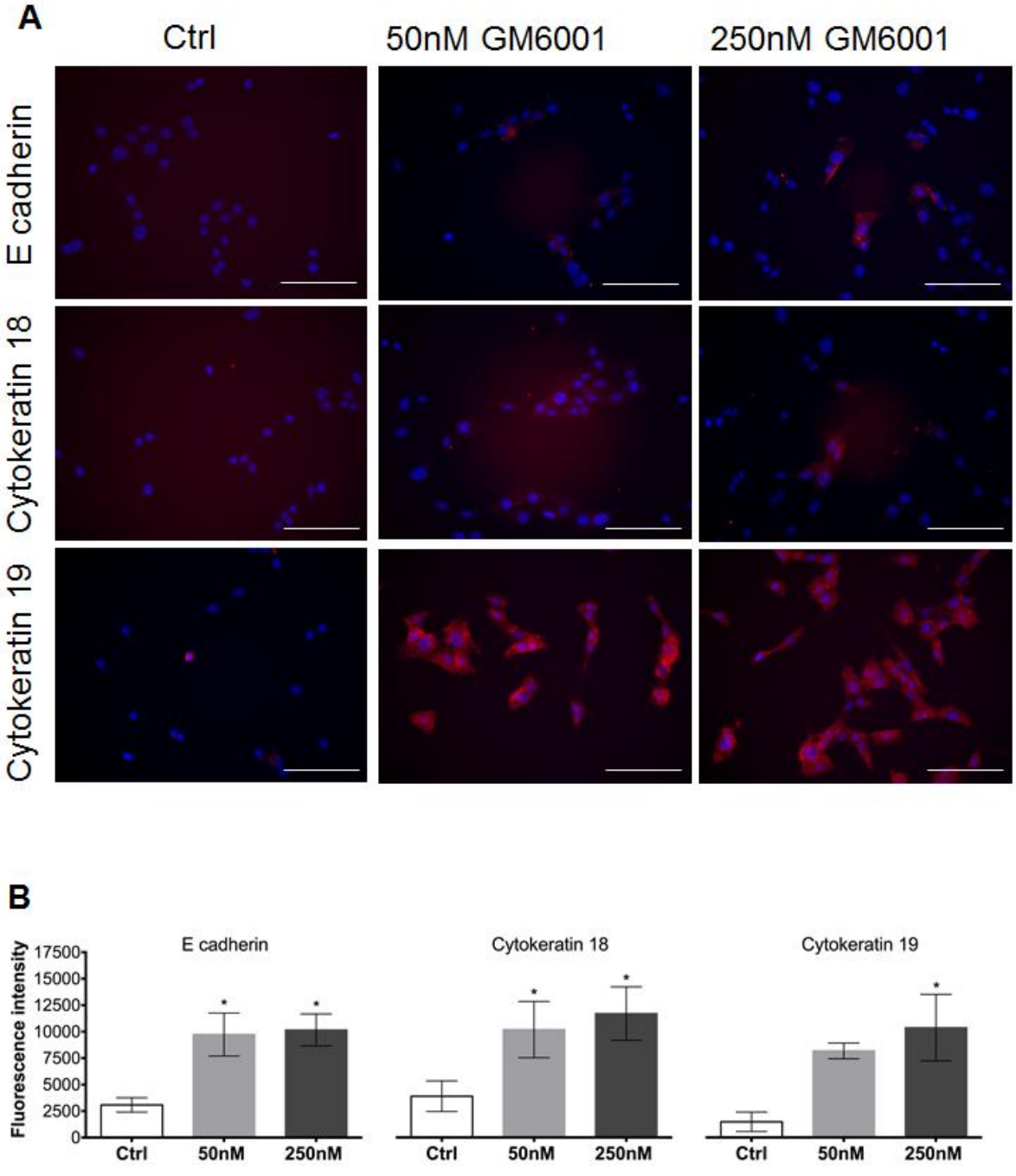

Figure 4: Alteration of the epithelial phenotype of MG63 sarcoma cells *in vitro*.

A) Immunofluorescence staining of the epithelial lineage protein E cadherin (red, 1st row), Cytokeratin 18 (red, 2nd row) and Cytokeratin 19 (red, 3rd row) in the control and treated MG63 cells. Nuclei were stained with DAPI. Scale bar = 100µm.

B) Quantification of protein expression through semi-automated image analysis for E cadherin, Cytokeratin 18 and Cytokeratin 19. Images were taken from 3 biological replicates, and the median fluorescence intensities of Fibronectin and α SMA were determined. *P<0.05.

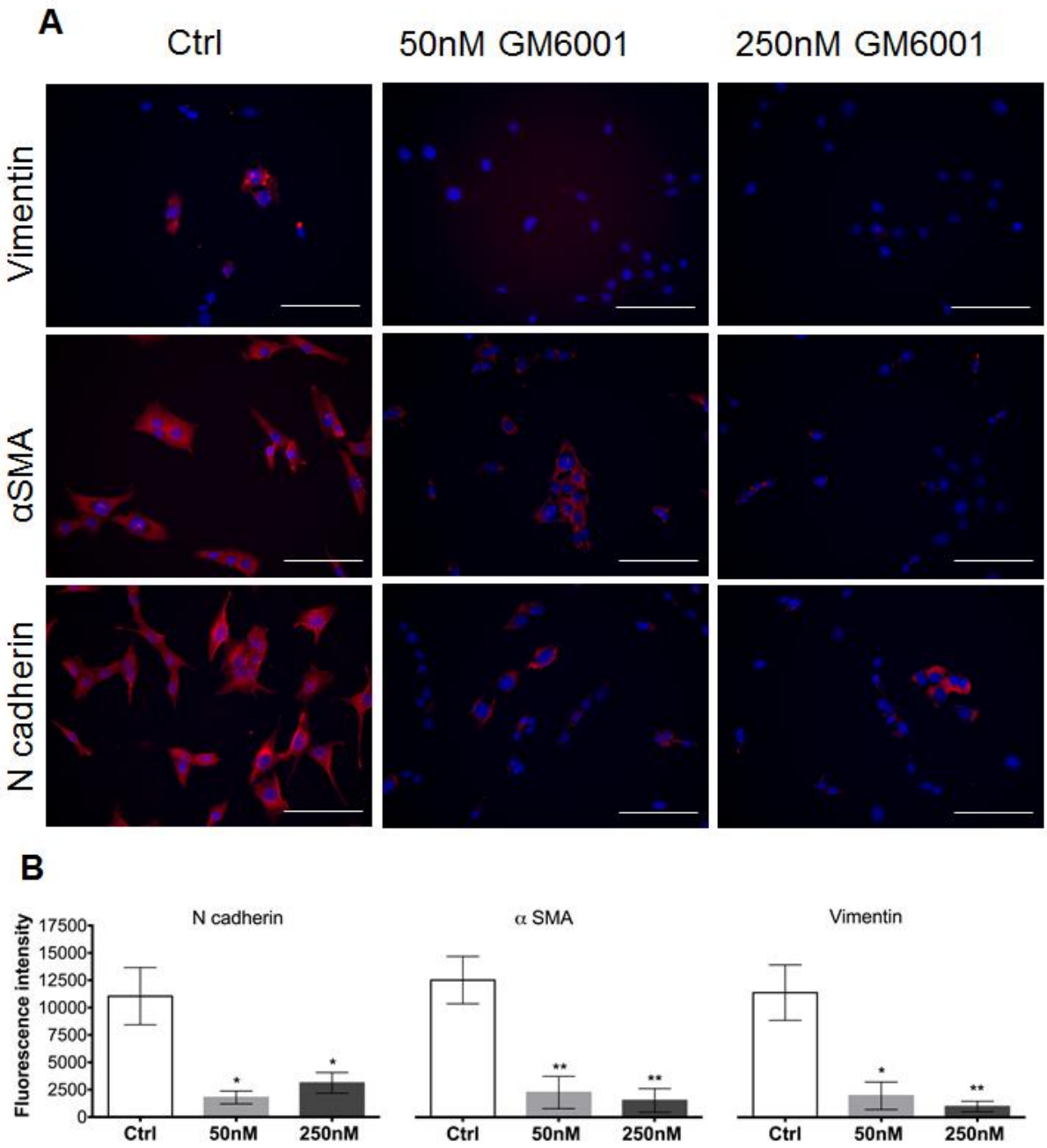

Figure 5: Alteration of the mesenchymal phenotype of MG63 sarcoma cells *in vitro*.
A) Immunofluorescence staining of the mesenchymal lineage protein Vimentin (red, 1st row), α-smooth muscle actin (α SMA) (red, 2nd row) and N cadherin (red, 3rd row) in the control and treated MG63 cells. Nuclei were stained with DAPI. Scale bar = 100μm. **B)** Quantification of protein expression through semi-automated image analysis for Vimentin, α SMA and N cadherin. Images were taken from 3 biological replicates, and the median fluorescence intensities of Fibronectin and α SMA were determined. *P<0.05 and **P<0.01.

MMP Inhibition Effects the Cell Migration of MG63 Cells *in vitro*

To further investigate the effect of MMP inhibition on the sarcoma cell line, time-lapse video microscopy was used to examine the migration pathways of MG63 cells under the different treatments. Cells were administered with 50nM and 250nM GM6001 for 12 hours, and then immediately subjected to video imaging. All of the actual cell trajectories from each of the different groups were obtained from a 6-hour period where the data was pooled from 3 experiments (Figure 6 A). The trajectories of the GM6001 treated MG63 cells migrated significantly shorter than the control untreated cells. Quantitative analysis of the single cell migration path (Figure 6 B) revealed a significantly decreased net translocation distance (straight distance from the cell's origin to the end point) for MG63 that received GM6001 treatment. There was no significant difference between the 2 tested concentrations.

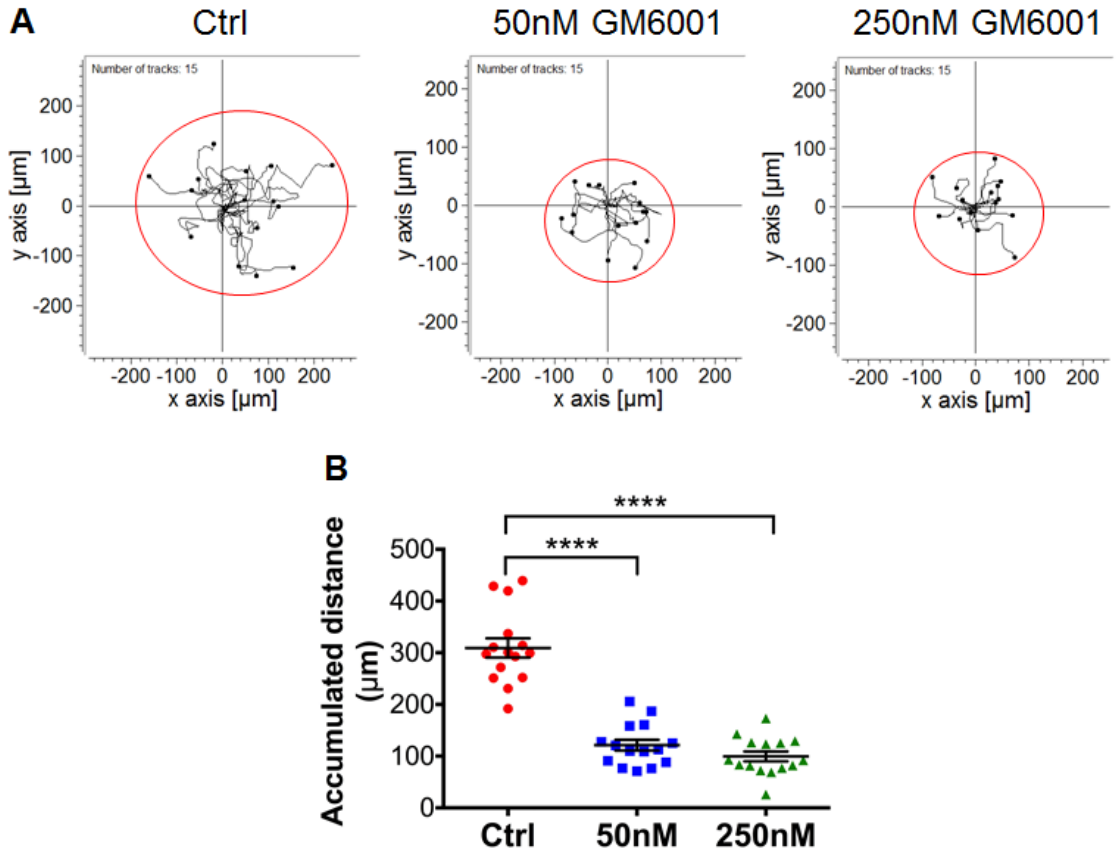

Figure 6: Single cell migration of MG63 cells *in vitro*.
A) Single cell migration pathways of the control and MMP inhibitor treated MG63 cells. The migration paths of 20 individual cells of different experimental groups were captured in a time-lapse motility assay. Data was pooled from 3 independent experiments. **B)** Graphs show the calculated accumulated distance of the cells. Data are represented as the mean ±SEM of 60 individual cells from 3 biological replicates. ****P<0.0001.

Discussion

A complex array of cellular proteins and molecules are slowly being elucidated to serve as markers for the EMT process[19, 20, 23, 24, 28-32, 34, 37-40]. Among these markers, a few have stood out to more specifically delineate the occurrence of the phenomenon. It is generally recognized that the loss of the epithelial marker E-cadherin and subsequent progression to increased mesenchymal expression, specifically of N-cadherin and Vimentin, plays a critical role in the process of EMT[28, 31, 37, 38]. E-cadherin is a cell surface adhesion protein that localizes in the apical-lateral junction between membranes. Because polarized membranes are essentially for this localization of E-cadherin, it is generally thought that epithelial cells expressing E-cadherin express some form of apical basal polarity, and thus it logically follows that E-cadherin expression must be repressed in order for EMT to occur[31, 37]. Its expression is mediated by various transcription factors, including SNAIL[38]. N-cadherin is a key embryogenic adhesion molecule and is associated with the mesenchymal phenotype. It is intimately involved in multiple signaling pathways, including tyrosine kinase signaling through fibroblast growth factor receptor and Rho GTPase signaling[41]. It has therefore been inferred that cancers with high levels of N-cadherin expression and low levels of E-cadherin expression have poorer prognoses. Indeed, prostate cancer patients with high levels of N-cadherin expression and low levels of E-cadherin expression experienced significantly higher rates of adverse clinical events[42, 43].

In accordance to the literature, undifferentiated MG63 cells highly expressed several MMPs, such as MMP1, MMP2, MMP3, MMP9 and MMP14 as shown by our qPCR analysis. However, we did not see any expression of MMP7, MMP8, MMP12 and MMP26 in our cultured cells. The treatment of the MMP inhibitor downregulated the gene expression of all the tested MMPs with the exception of MMP12.

MMP inhibition resulted in subsequent attenuation of mesenchymal gene and protein expression in human osteosarcoma cells. While the cells never expressed E-cadherin and Cytokeratins at baseline, the inhibition of MMPs significantly increased their expression, while the expression of N-cadherin was attenuated, the elevation of which has been independently found to cause increased rates of adverse clinical events in patients. We also saw adecreased expression of the other tested mesenchymal α-SMA and Vimentin upon MMP inhibition.

This is particularly intriguing considering Vimentin's expression particularly in osteoblast cells. These data may suggest a regression and possible switching of lineages from a mesenchymal to a more epithelioid nature upon the addition of MMP inhibitor, a finding that is consistent with that observed in the literature[4, 15, 34].

Moreover, cells that were treated with MMP inhibitor also subsequently showed significantly decreased migratory capacity, a finding that is again consistent with the literature [4, 10, 14, 15]. Cellular tracking of this process showed significant decreases in the osteosarcoma migratory distance in the presence of MMP inhibitor, the GM6001.

While this does not definitively prove the link between the loss of mesenchymal phenotype and attenuated migratory potential, it supports the relationship between the two variables. Further work should be done to see if replacement of key mesenchymal factors in the presence of MMPinhibition restores the migratory potential of cells. It would also be interesting to further investigate the link between MMPinhibition, mesenchymal phenotype, and subsequent chemotherapy resistance, particularly to see if the inhibition of MMPs decreases cellular threshold tolerance of these cells to chemotherapeutic agents and widens the therapeutic window. Further studies should include the animal models to clarify these discoveries.

Our study suggests that perhaps the simultaneous presence of attenuated mesenchymal phenotype and decreased migratory potential in the presence of MMP inhibition may provide additional mechanistic evidence and a novel perspective when examining MMP inhibition in cancer cells. Evidence for this potential linkage has existed in the literature for years[3, 4, 10, 14, 15]. MET is certainly one important potential mechanism for this phenomenon. One potential explanation for why MMPinhibition causes loss of mesenchymal phenotype can be found in the realm of cellular engineering. It has recently been discovered that when differentiated cells are unable to attach to the extra cellular matrix, they regress along the embryonic lineage and begin to exhibit a more stem-like phenotype. It has been suggested that this may be a survival mechanism. MMPs have long been known to degrade the extra cellular matrix and sever these connections and its involvement in EMT processes is crucial (Figure 7). It therefore follows that inhibition of this process may prevent the gain of stem-like qualities while inhibiting pivotal migratory processes. In conclusion, while much is known about the involvement of MMPs in malignant processes, it is clear that there is still much to be examined. These data may provide evidence for a novel perspective regarding the role of MMPs in MET processes and migratory potential.

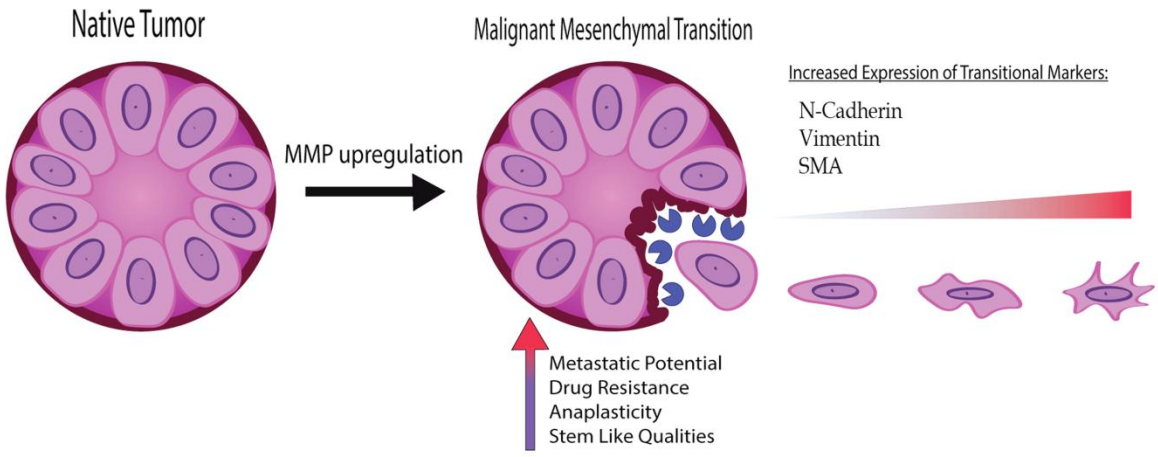

Figure 7: The role of MMPs in mesenchymal-epithelial transitional processes of tumor cells.
Schematic illustration of the role of MMP upregulation in the malignant mesenchymal transition processes in tumor cells. MMP upregulation increases the expression of transitional markers, such as N-Cadherin, Vimentin, and α-smooth muscle actin (SMA). This results in increased tumor metastatic potential, drug resistance, anaplasticity and stem cell like qualities.

Acknowledgements

This work was supported by the CPRIT shared instrumentation grant (to Y.L.), Institute of Molecular Medicine, University of Texas Health Science Center at Houston, USA; the Dean's Grant from the University of Texas Medical School at Houston, and a grant from the Department of Nanomedicine and Bioengineering at the University of Texas Health Science Center at Houston (to C.F.)

References

1. Davis AM, Bell RS and Goodwin PJ. Prognostic factors in osteosarcoma: a critical review. J Clin Oncol 1994; 12: 423-431.
2. Jaffe N. Osteosarcoma: review of the past, impact on the future. The American experience. Cancer Treat Res 2009; 152: 239-262.
3. Bellayr I, Holden K, Mu X, Pan H and Li Y. Matrix metalloproteinase inhibition negatively affects muscle stem cell behavior. Int J Clin Exp Pathol 2013; 6: 124-141.
4. Brown PD and Giavazzi R. Matrix metalloproteinase inhibition: a review of anti-tumour activity. Ann Oncol 1995; 6: 967-974.
5. Chen X and Li Y. Role of matrix metalloproteinases in skeletal muscle: migration, differentiation, regeneration and fibrosis. Cell Adh Migr 2009; 3: 337-341.
6. Huntington JT, Shields JM, Der CJ, Wyatt CA, Benbow U, Slingluff CL, Jr. and Brinckerhoff CE. Overexpression of collagenase 1 (MMP-1) is mediated by the ERK pathway in invasive melanoma cells: role of BRAF mutation and fibroblast growth factor signaling. J Biol Chem 2004; 279: 33168-33176.
7. Kotiyal S and Bhattacharya S. Breast cancer stem cells, EMT and therapeutic targets. Biochem Biophys Res Commun 2014; 453: 112-116.
8. Pytliak M, Vargova V and Mechirova V. Matrix metalloproteinases and their role in oncogenesis: a review. Onkologie 2012; 35: 49-53.
9. Qian Q, Wang Q, Zhan P, Peng L, Wei SZ, Shi Y and Song Y. The role of matrix metalloproteinase 2 on the survival of patients with non-small cell lung cancer: a systematic review with meta-analysis. Cancer Invest 2010; 28: 661-669.
10. Rasmussen HS and McCann PP. Matrix metalloproteinase inhibition as a novel anticancer strategy: a review with special focus on batimastat and marimastat. Pharmacol Ther 1997; 75: 69-75.
11. Wang W, Pan H, Murray K, Jefferson BS and Li Y. Matrix metalloproteinase-1 promotes muscle cell migration and differentiation. Am J Pathol 2009; 174: 541-549.
12. Guo Y, Zi X, Koontz Z, Kim A, Xie J, Gorlick R, Holcombe RF and Hoang BH. Blocking Wnt/LRP5 signaling by a soluble receptor modulates the epithelial to mesenchymal transition and suppresses met and metalloproteinases in osteosarcoma Saos-2 cells. J Orthop Res 2007; 25: 964-971.
13. Hazan RB, Qiao R, Keren R, Badano I and Suyama K. Cadherin switch in tumor progression. Ann N Y Acad Sci 2004; 1014: 155-163.
14. Kontogiorgis CA, Papaioannou P and Hadjipavlou-Litina DJ. Matrix metalloproteinase inhibitors: a review on pharmacophore mapping and (Q)SARs results. Curr Med Chem 2005; 12: 339-355.
15. Watson SA and Tierney G. Matrix metalloproteinase inhibitors: a review. BioDrugs 1998; 9: 325-335.
16. Yang X, Wang YP, Liu FX, Zeng K, Qian MQ, Chen G, Shi L and Zhu GX. Increased invasiveness of osteosarcoma mesenchymal stem cells induced by bone-morphogenetic protein-2. In Vitro Cell Dev Biol Anim 2013; 49: 270-278.
17. Zhang D, Bar-Eli M, Meloche S and Brodt P. Dual regulation of MMP-2 expression by the type 1 insulin-like growth factor receptor: the phosphatidylinositol 3-kinase/Akt and Raf/ERK pathways transmit opposing signals. J Biol Chem 2004; 279: 19683-19690.
18. Findlay VJ, Wang C, Watson DK and Camp ER. Epithelial-to-mesenchymal transition and the cancer stem cell phenotype: insights from cancer biology with therapeutic implications for colorectal cancer. Cancer Gene Ther 2014; 21: 181-187.
19. Kalluri R and Weinberg RA. The basics of epithelial-mesenchymal transition. J Clin Invest 2009; 119: 1420-1428.
20. Gurzu S, Ciortea D, Munteanu T, Kezdi-Zaharia I and Jung I. Mesenchymal-to-endothelial transition in Kaposi sarcoma: a histogenetic hypothesis based on a case series and literature review. PLoS One 2013; 8: e71530.
21. Roodhart JM, Daenen LG, Stigter EC, Prins HJ, Gerrits J, Houthuijzen JM, Gerritsen MG, Schipper HS, Backer MJ, van Amersfoort M, Vermaat JS, Moerer P, Ishihara K, Kalkhoven E, Beijnen JH, Derksen PW, Medema RH, Martens AC,

Brenkman AB and Voest EE. Mesenchymal stem cells induce resistance to chemotherapy through the release of platinum-induced fatty acids. Cancer Cell 2011; 20: 370-383.

22. Tsukamoto S, Honoki K, Fujii H, Tohma Y, Kido A, Mori T, Tsujiuchi T and Tanaka Y. Mesenchymal stem cells promote tumor engraftment and metastatic colonization in rat osteosarcoma model. Int J Oncol 2012; 40: 163-169.
23. Bian ZY, Fan QM, Li G, Xu WT and Tang TT. Human mesenchymal stem cells promote growth of osteosarcoma: involvement of interleukin-6 in the interaction between human mesenchymal stem cells and Saos-2. Cancer Sci 2010; 101: 2554-2560.
24. Machado I, Lopez-Guerrero JA, Navarro S, Alberghini M, Scotlandi K, Picci P and Llombart-Bosch A. Epithelial cell adhesion molecules and epithelial mesenchymal transition (EMT) markers in Ewing's sarcoma family of tumors (ESFTs). Do they offer any prognostic significance? Virchows Arch 2012; 461: 333-337.
25. Martins-Neves SR, Lopes AO, do Carmo A, Paiva AA, Simoes PC, Abrunhosa AJ and Gomes CM. Therapeutic implications of an enriched cancer stem-like cell population in a human osteosarcoma cell line. BMC Cancer 2012; 12: 139.
26. Niinaka Y, Harada K, Fujimuro M, Oda M, Haga A, Hosoki M, Uzawa N, Arai N, Yamaguchi S, Yamashiro M and Raz A. Silencing of autocrine motility factor induces mesenchymal-to-epithelial transition and suppression of osteosarcoma pulmonary metastasis. Cancer Res 2010; 70: 9483-9493.
27. Xiao W, Mohseny AB, Hogendoorn PC and Cleton-Jansen AM. Mesenchymal stem cell transformation and sarcoma genesis. Clin Sarcoma Res 2013; 3: 10.
28. Yang J, Du X, Wang G, Sun Y, Chen K, Zhu X, Lazar AJ, Hunt KK, Pollock RE and Zhang W. Mesenchymal to epithelial transition in sarcomas. Eur J Cancer 2014; 50: 593-601.
29. Bonuccelli G, Avnet S, Grisendi G, Salerno M, Granchi D, Dominici M, Kusuzaki K and Baldini N. Role of mesenchymal stem cells in osteosarcoma and metabolic reprogramming of tumor cells. Oncotarget 2014; 5: 7575-7588.
30. Cates JM, Dupont WD, Barnes JW, Edmunds HS, Fasig JH, Olson SJ and Black CC. Markers of epithelial-mesenchymal transition and epithelial differentiation in sarcomatoid carcinoma: utility in the differential diagnosis with sarcoma. Appl Immunohistochem Mol Morphol 2008; 16: 251-262.
31. Gravdal K, Halvorsen OJ, Haukaas SA and Akslen LA. A switch from E-cadherin to N-cadherin expression indicates epithelial to mesenchymal transition and is of strong and independent importance for the progress of prostate cancer. Clin Cancer Res 2007; 13: 7003-7011.
32. Hou CH, Lin FL, Hou SM and Liu JF. Cyr61 promotes epithelial-mesenchymal transition and tumor metastasis of osteosarcoma by Raf-1/MEK/ERK/Elk-1/TWIST-1 signaling pathway. Mol Cancer 2014; 13: 236.
33. Karnuth B, Dedy N, Spieker T, Lawlor ER, Gattenlohner S, Ranft A, Dirksen U, Jurgens H and Brauninger A. Differentially expressed miRNAs in Ewing sarcoma compared to mesenchymal stem cells: low miR-31 expression with effects on proliferation and invasion. PLoS One 2014; 9: e93067.
34. Kramer K, Hicks DG, Palis J, Rosier RN, Oppenheimer J, Fallon MD and Cohen HJ. Epithelioid osteosarcoma of bone. Immunocytochemical evidence suggesting divergent epithelial and mesenchymal differentiation in a primary osseous neoplasm. Cancer 1993; 71: 2977-2982.
35. NguyenThai QA, Sharma N, Luong DH, Sodhi SS, Kim JH, Kim N, Oh SJ and Jeong DK. Targeted inhibition of osteosarcoma tumor growth by bone marrow-derived mesenchymal stem cells expressing cytosine deaminase/5-fluorocytosine in tumor-bearing mice. J Gene Med 2015;
36. Oliveras-Ferraros C, Corominas-Faja B, Cufi S, Vazquez-Martin A, Martin-Castillo B, Iglesias JM, Lopez-Bonet E, Martin AG and Menendez JA. Epithelial-to-mesenchymal transition (EMT) confers primary resistance to trastuzumab (Herceptin). Cell Cycle 2012; 11: 4020-4032.
37. Qian X, Anzovino A, Kim S, Suyama K, Yao J, Hulit J, Agiostratidou G, Chandiramani N, McDaid HM, Nagi C, Cohen HW, Phillips GR, Norton L and Hazan RB. N-cadherin/FGFR promotes metastasis through epithelial-to-mesenchymal transition and stem/progenitor cell-like properties. Oncogene 2014; 33: 3411-3421.

38. Saito T, Nagai M and Ladanyi M. SYT-SSX1 and SYT-SSX2 interfere with repression of E-cadherin by snail and slug: a potential mechanism for aberrant mesenchymal to epithelial transition in human synovial sarcoma. Cancer Res 2006; 66: 6919-6927.
39. Shang Y, Li Z, Li H, Xia H and Lin Z. TIM-3 expression in human osteosarcoma: Correlation with the expression of epithelial-mesenchymal transition-specific biomarkers. Oncol Lett 2013; 6: 490-494.
40. Tang J, Shen L, Yang Q and Zhang C. Overexpression of metadherin mediates metastasis of osteosarcoma by regulating epithelial-mesenchymal transition. Cell Prolif 2014; 47: 427-434.
41. Derycke LD and Bracke ME. N-cadherin in the spotlight of cell-cell adhesion, differentiation, embryogenesis, invasion and signalling. Int J Dev Biol 2004; 48: 463-476.
42. Umbas R, Isaacs WB, Bringuier PP, Schaafsma HE, Karthaus HF, Oosterhof GO, Debruyne FM and Schalken JA. Decreased E-cadherin expression is associated with poor prognosis in patients with prostate cancer. Cancer Res 1994; 54: 3929-3933.
43. Umbas R, Schalken JA, Aalders TW, Carter BS, Karthaus HF, Schaafsma HK, Debruyne FM and Isaacs WB. Expression of the cellular adhesion molecule E-cadherin is reduced or absent in high-grade prostate cancer. Cancer Res 1992; 52: 5104-5109.